Available online at www.sciencedirect.com
ScienceDirect
Dyes and Pigments 75 (2007) 136–142
DYES and PIGMENTS
www.elsevier.com/locate/dyepig

Removal of cyanocobalamine from aqueous solution using mesoporous activated carbon

Ewa Lorenc-Grabowska, Grażyna Gryglewicz*

Faculty of Chemistry, Department of Polymer and Carbonaceous Materials, Wrocław University of Technology, ul. Gdańska 7/9, 50-344 Wrocław, Poland

Received 20 April 2006; received in revised form 23 May 2006; accepted 24 May 2006
Available online 11 July 2006

Abstract

The adsorption of cyanocobalamine was studied using coal-based mesoporous activated carbon (AC). The ACs tested showed a comparable pore volume, around 0.5 $cm^3 g^{-1}$, but different contribution of mesopores ranging from 0.53 to 0.82 $cm^3 g^{-1}$. The adsorption of cyanocobalamine was carried out in slightly alkaline solution in static conditions. Three kinetic models including a first-order Lagergren model, a pseudo-second-order model, and an intraparticle diffusion model were applied to describe the kinetics and mechanism of adsorption. The adsorption of cyanocobalamine on mesoporous carbons followed the pseudo-second-order model. The diffusion of cyanocobalamine molecule within smaller mesopores was identified to be the rate-limiting step. The analysis of adsorption equilibrium data indicates that the adsorption of cyanocobalamine better fits the Langmuir equation than the Freundlich equation. The Langmuir adsorption capacity of the carbon is strongly related to the degree of mesoporosity development. Among ACs tested, the carbon with the highest mesopore volume and mesopore width of 10–50 nm shows the greater ability to remove cyanocobalamine from aqueous solution. The effect of pore-size distribution on the kinetics and mechanism of adsorption has been discussed.

Keywords: Adsorption; Cyanocobalamine; Activated carbon; Kinetics

1. Introduction

Many industries consume large amounts of water in manufacturing processes and, simultaneously, release a huge amount of wastewater. Dyes and pigments represent a group of easily detected colored compounds that are emitted to the environment from various industries such as dye manufacturing, textile finishing, food coloring, cosmetics, pharmaceutics and others [1]. Color is usually the first contaminant to be considered in wastewater; some dyes can pose a health risk to humans. Moreover, discharging of dyes into water resources even in a small amount can affect aquatic life. Generally, dyes are difficult to remove by conventional treatment methods due to their nonbiodegradable nature and their resistance to degradation by light and oxidizing agents [2–4].

In recent years adsorption processes have been found to be successful in the treatment of colored organic effluent [5–9]. Activated carbons (ACs) are the most common adsorbents commercially used for the removal of organic compounds from water streams. The removal efficiency of a given adsorbent is mainly related to the pore-size distribution and the size of the adsorbate molecule. Other factors, such as surface properties of adsorbent, chemical structure of adsorbate and solution pH, are also very important because they have an influence on the interactions between the surface of adsorbent and the adsorbed molecule [10,11]. Most commercially available ACs are microporous showing high efficiency for the removal of low molecular weight compounds [11–13]. For efficient removal of large molecules, the ACs with well-developed mesopore structure (pore size of 2–50 nm) are

* Corresponding author. Fax: +48 71 3221580.
E-mail address: grazyna.gryglewicz@pwr.wroc.pl (G. Gryglewicz).

0143-7208/$ - see front matter © 2006 Elsevier Ltd. All rights reserved.
doi:10.1016/j.dyepig.2006.05.023

recommended. The molecular dimensions for some dyes and pigments are close to upper limit of micropore size and even exceed 2 nm. However, there is only limited research on the adsorption of large molecules by mesoporous ACs [14–16]. Moreover, the kinetics and mechanism of adsorption is often studied without paying attention to the porous texture of adsorbent used, in particular, the pore volume distribution [5,7,17,18].

The ACs based on agricultural solid wastes have recently been used to remove a number of dyes from aqueous solution [19–23]. However, in some cases the adsorption capacity of these adsorbents was not large mainly due to their low mesopore volume. A much higher efficiency in the removal of dyes, such as Congo Red, could be achieved using bituminous coal-based mesoporous carbon [24].

In this work the adsorption of cyanocobalamine on the ACs of different extent of mesoporosity was studied. This particular colored compound, Vitamin B_{12}, can occur in wastewater from the pharmaceutical industry. The cyanocobalamine molecule can be considered as large in terms of size (1.84 nm; 1.41 nm; 1.14 nm) and M_r (1355) [14]. The effect of both the mesopore volume and the pore-size distribution of carbons on the removal degree of cyanocobalamine from aqueous solution was determined. The mechanism of the adsorption on mesoporous activated carbons have been also discussed using different models describing the adsorption from solution.

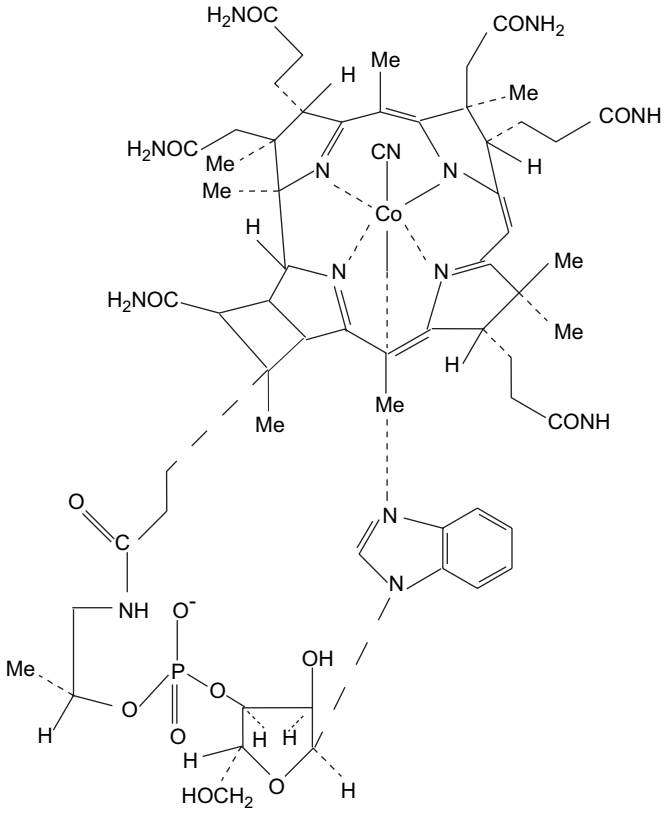

Fig. 1. Molecular structure of cyanocobalamine [14].

2. Experimental

2.1. Materials

Three ACs with different mesopore fraction were prepared using subbituminous coal (subA) from Kazimierz–Juliusz (KJ) mine as starting material. All the activated carbons were produced by carbonization at 850 °C and steam activation at the same temperature up to 50% burn-off. Prior to heat treatment, the initial coal was loaded with calcium and iron by ion exchange according to the procedure reported elsewhere [25]. The oxidation with nitric acid (N) or sulfonation with sulfuric acid (S) was used for the generation of ion-exchangeable groups on the coal surface. The activated carbons obtained as described above are designed as KJA/N/CaFe and KJA/S/CaFe. The KJA/Ti carbon was produced by activation of the KJ coal impregnated with acetylacetonate titanium oxide $TiO(acac)_2$ [26]. The percentage, by mass, of Ti to coal was 2.5%.

For adsorption studies cyanocobalamine purchased from Fluka was used as adsorbate; the molecular structure of cyanocobalamine is shown in Fig. 1.

2.2. Adsorption test

The adsorption process of cyanocobalamine from aqueous solution was carried out at 25 °C in a static system. A sieve fraction of activated carbon between 0.2 and 0.5 mm was used for the sorption experiments. The carbon sample was washed with deionised water and dried at 105–110 °C for 24 h before use. To establish the equilibrium time, 0.2 g of activated carbon was placed into the set of flasks that were kept in a thermostat shaker bath and agitated for 4 days. For the adsorption isotherm determination, 0.01–0.2 g of activated carbon was placed into Erlenmeyer flasks and 0.1 dm^3 of adsorbate solution (50 mg dm^{-3}) was added into each of the flasks. Each set of flasks included two additional flasks containing blank solution to check the adsorption of sorbate on the walls. The stoppered flasks were kept in a thermostat shaker bath and agitated for 2 days. Before and after contact, the pH of solutions was measured by a digital pH-meter (Accumet Basic, Fisher Scientific) using a glass electrode.

2.3. Analyses

The porous structure parameters of the activated carbons were determined from benzene adsorption at 25 °C in a McBain apparatus for gravimetric sorption measurements. Specific surface area S_{BET} was taken from benzene adsorption isotherms using BET equation. The Gurvitch rule and Kelvin condensation theory were used to establish the extent of microporosity and the mesopore volume distribution, respectively [27]. The amount of benzene adsorbed at the relative pressure of $p\,p_0^{-1} = 0.96$ was employed to determine the total pore volume which corresponds to the sum of the micropore and mesopore volumes. The micropore volume (V_{mic}) was

calculated as a difference between the total pore volume (V_{tot}) and mesopore volume (V_{mes}) calculated from Kelvin equation. Assuming the pores to be parallel and cylindrical, the mean pore width was calculated on the basis of BET surface area and total pore volume. The calculated mesopore fraction is the ratio of mesopore volume to the total pore volume (V_{mes}/V_{tot}). The concentration of solute remaining in the water phase was measured using a spectrophotometer at wavelength 361 nm.

3. Result and discussion

3.1. Characteristics of ACs

The adsorption–desorption isotherms of benzene for the ACs are presented in Fig. 2. The shape of isotherms of all carbons proves their mesoporous nature. An enlarged hysteresis loop in the order KJA/Ti < KJA/S/CaFe < KJA/N/CaFe can be observed that reflects an increasing amount of mesopores in the porous texture of carbons used. The porous structure parameters of ACs calculated from their corresponding isotherms are given in Table 1. The carbons are characterized by the total pore volume in the range of 0.505–0.525 $cm^3 g^{-1}$ and the mesopore fraction between 0.53 and 0.82. The BET surface area ranges from 331 to 679 $m^2 g^{-1}$. An increase in the mesopore volume from 0.271 to 0.427 $cm^3 g^{-1}$ is accompanied by widening of pore width from 2.98 to 6.28 nm. The mesopore volume distribution of the ACs used is shown in Fig. 3. It can be seen that the mesopores in size range of 2–5 nm are predominant for KJA/S/CaFe whereas wider mesopores, between 10 and 50 nm, have the largest contribution to the porous texture of KJA/N/CaFe. In the case of KJA/Ti micropores constitute a half of the porous texture.

Table 1
Porous texture characteristics of ACs tested

Activated carbons	S_{BET} ($m^2 g^{-1}$)	V_{tot} ($cm^3 g^{-1}$)	V_{mic} ($cm^3 g^{-1}$)	V_{mes} ($cm^3 g^{-1}$)	Mesopore fraction	Mean pore width (nm)
KJA/N/CaFe	331	0.520	0.093	0.427	0.82	6.28
KJA/S/CaFe	475	0.525	0.122	0.403	0.76	4.42
KJA/Ti	679	0.505	0.234	0.271	0.53	2.98

3.2. Adsorption

3.2.1. Adsorption tests

The adsorption process depends on the porous texture and surface chemistry of the adsorbent, the nature of the adsorbate (e.g. molecular size, polarity, solubility) and the process conditions such as solution pH and ionic strength and temperature [11,28–30]. In the case of organic pollutants, which in most cases are weak electrolytes, both electrostatic and dispersive interactions between the adsorbate molecule and the carbon surface can influence the adsorption process. In our case, the electrostatic forces can be neglected because cyanocobalamine occurs in the neutral form under conditions of adsorption test used in this work. Moreover, a high symmetry of adsorbate molecule minimizes the impact of polarizability on the extent of adsorption (inductive effect). Therefore, the dispersive interactions of van der Waals type seem to be dominant in the adsorption process of cyanocobalamine.

The extent of removal of cyanocobalamine by mesoporous carbons vs. time is shown in Fig. 4. The time needed to reach the equilibrium of adsorption decreases in the order KJA/Ti > KJA/S/CaFe > KJA/N/CaFe. This trend is consistent with an increase in the contribution of mesopores into the porous texture (Table 1). Approximately, 17 h is required to attain the equilibrium for KJA/N/CaFe whereas double longer time is found for KJA/Ti. It can be clearly seen that the equilibrium time is related to both the total mesopore volume and

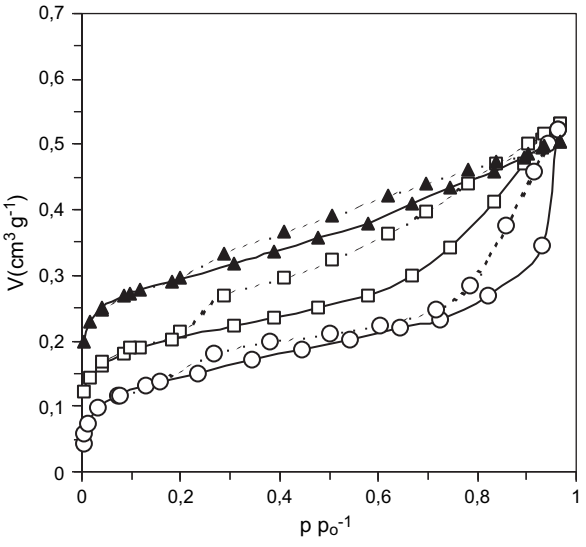

Fig. 2. Adsorption (—) and desorption (- - -) isotherms of benzene at 25 °C for activated carbons. ○, KJA/N/CaFe; □, KJA/S/CaFe; ▲, KJA/Ti.

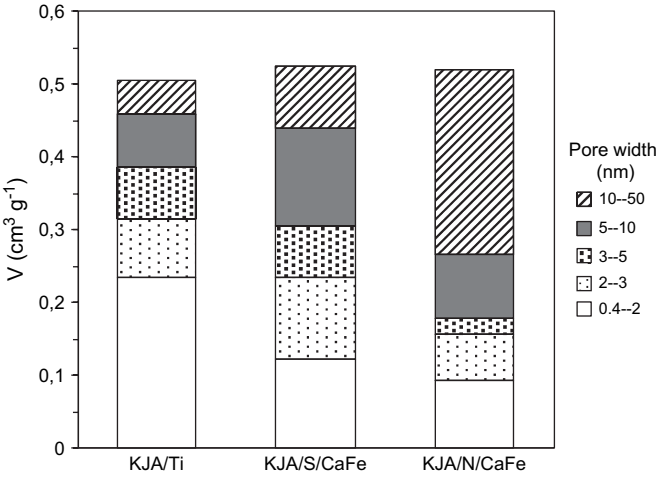

Fig. 3. Pore volume distribution of subbituminous coal-based mesoporous carbons.

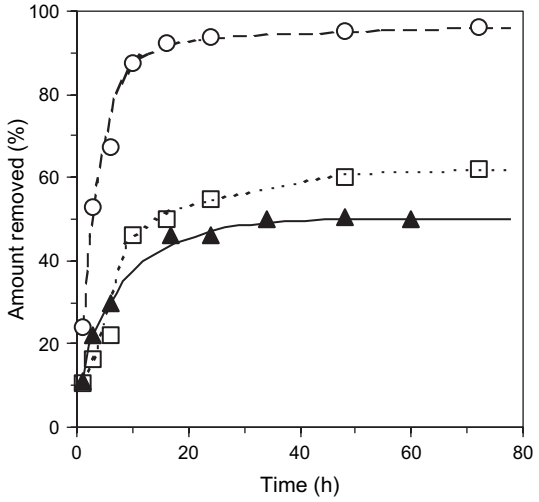

Fig. 4. Removal of cyanocobalamine by activated carbons as a function of time. ○, KJA/N/CaFe; □, KJA/S/CaFe; ▲, KJA/Ti.

the volume of mesopores with a size between 10 and 50 nm (Fig. 3). The higher the volume of larger mesopores, the shorter is the equilibrium time. It can be concluded that for conditions used the removal of cyanocobalamine is mainly determined by porous texture of the carbon.

The ACs differ in the percentage of cyanocobalamine adsorbed at equilibrium. The equilibrium uptake is the highest for KJA/N/CaFe, over 98%. KJA/S/CaFe removes about 62% of cyanocobalamine. The lowest uptake, only 49%, can be observed in the case of KJA/Ti. This indicates that the carbon with the highest mesopore volume shows the greatest efficiency in the removal of cyanocobalamine. Taking into account that the micropore volume of the carbons decreases in the direction as follows KJA/Ti > KJA/S/CaFe > KJA/N/CaFe, it can be deduced that the adsorption in the mesopores is mainly responsible for removing cyanocobalamine.

3.2.2. Adsorption kinetics

The kinetics of adsorption of cyanocobalamine from aqueous solution has been discussed in view of first-order Lagergren model, the pseudo-second-order model and the intraparticle diffusion model. The first-order Lagergren equation is given by Eq. (1) [7,31,32]:

$$\log\left(q_{e\,exp} - q_t\right) = \log q_e - k_1 t/2.303 \quad (1)$$

Pseudo-second-order model is described by Eq. (2) [20,31–33]:

$$t/q_t = 1/\left(k_2 q_e^2\right) + t/q_e \quad (2)$$

where t and q_t are, respectively, time (min) and the amount adsorbed by carbon at time t (mg g^{-1}). $q_{e\,exp}$ and q_e are the amount adsorbed at equilibrium-experimental data and equilibrium-calculated data, respectively, expressed as mg g^{-1} sample. k_1 and k_2 are the first (min^{-1}) and second (g min^{-1} mg^{-1}) order rate constant of adsorption. The calculated results for both models are given in Table 2. It can be noted that the correlation coefficient (R^2) for the first-order equation is low, ranging from 0.708 to 0.945. Moreover, for two of three carbons studied the experimental $q_{e\,exp}$ value does not agree well with the calculated q_e value. A very good agreement between the $q_{e\,exp}$ and q_e values can be observed when the pseudo-second-order kinetic model was applied. Fig. 5 shows the straight-line plots of t/q_t vs. t for different mesoporous carbons. In this case, the correlation coefficients are very high, between 0.989 and 0.999. These results indicate that the adsorption of cyanocobalamine on mesoporous carbons obeys the pseudo-second-order kinetic model. The values of the rate constant k_2 were found to decrease with increasing both the mean pore width and the mesopore contribution to the porous texture.

The adsorption process in porous materials can be separated into three stages. The first stage is external diffusion or boundary layer diffusion of solute molecules. The second step is diffusion within the pores of the adsorbent internal structure to the sorption sites. The third stage includes very fast adsorption of molecule on active sites of the surface. Therefore, two former stages can control the adsorption rate. In many reports on the dyes adsorption the intraparticle diffusion is considered as the rate-limiting stage, however, boundary layer diffusion can also control the adsorption process in the initial stage to some extent [32,33]. This model is given by the following equation, Eq. (3):

$$q_t = k_p t^{1/2} \quad (3)$$

where q_t and k_p are the amount adsorbed at time t (mg g^{-1}) and intraparticle rate constant (mg g^{-1} min$^{-1/2}$), respectively. Fig. 6 shows the fractional uptake q_t as a function of $t^{1/2}$ for the adsorption of cyanocobalamine on mesoporous ACs. It can be clearly seen that the plots are composed of two linear parts. The first linear plot passes through (0,0) indicating that the boundary layer diffusion does not control the rate of cyanocobalamine adsorption. Therefore, in this case the intraparticle diffusion is the only rate-controlling step. The intraparticle diffusion is likely to occur in two stages. At first, cyanocobalamine molecules enter the macropores and wider mesopores that play the role as transporting arteries. Then,

Table 2
Comparison of the first-order and pseudo-second-order kinetics models of cyanocobalamine adsorption

Activated carbons	First-order kinetic model				Second-order kinetic model		
	$q_{e\,exp}$ (mg g^{-1})	q_e (mg g^{-1})	k_1 (min^{-1})	R^2	q_e (mg g^{-1})	k_2 (g mg^{-1} min^{-1})	R^2
KJA/N/CaFe	48	19	0.094	0.938	50	1.5×10^{-5}	0.999
KJA/S/CaFe	31	33	0.101	0.945	35	6.2×10^{-5}	0.989
KJA/Ti	25	36	0.009	0.708	27	1.5×10^{-4}	0.998

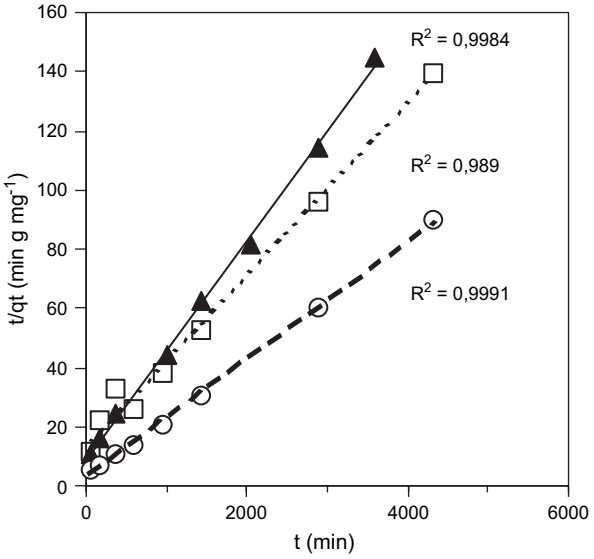

Fig. 5. Pseudo-second-order sorption kinetics of cyanocobalamine on mesoporous carbons. ○, KJA/N/CaFe; □, KJA/S/CaFe; ▲, KJA/Ti.

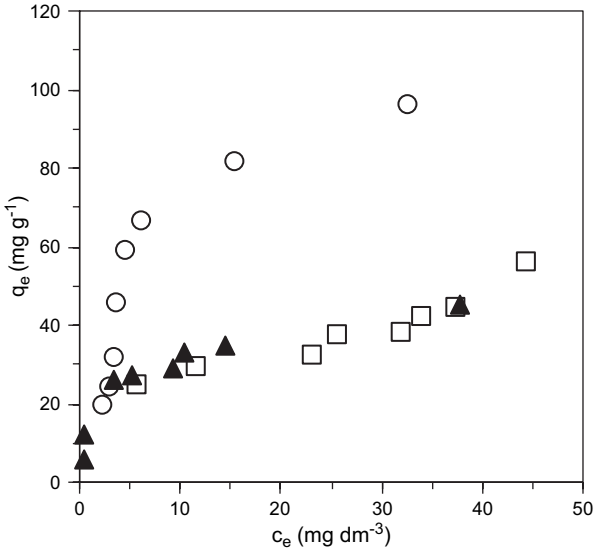

Fig. 7. Adsorption isotherms for cyanocobalamine on mesoporous carbons. ○, KJA/N/CaFe; □, KJA/S/CaFe; ▲, KJA/Ti.

the adsorbate molecule enters smaller mesopores more slowly that reflects a lower slope of the second linear part compared to the first linear part. This suggests that the diffusion within smaller mesopores is the rate determining-step in the adsorption process of cyanocobalamine. Moreover, for all carbons studied the slope of the second part of plot is nearly parallel indicating a comparable rate of adsorption in smaller mesopores, whereas there is a difference between carbons in the slope of the first portion of plots. As can be seen in Fig. 6 this slope increases in the order KJA/Ti < KJA/S/CaFe < KJA/N/CaFe that may reflect an enhanced diffusion of cyanocobalamine molecule through the macropores and wider mesopores.

3.2.3. Adsorption isotherms

Fig. 7 shows the adsorption isotherms for cyanocobalamine on three mesoporous carbons. The time taken to attain the equilibrium was 48 h for all carbons. The equilibrium-experimental data were interpreted using Langmuir and Freundlich equations that are most frequently applied in the study on the adsorption from an aqueous solution. The Langmuir isotherm is represented by Eq. (4):

$$q_e = (bq_{max}c_e)/(1 + bc_e) \quad (4)$$

where q_e is the equilibrium concentration on the adsorbent (mg g^{-1}), c_e is the equilibrium concentration in solution (mg dm^{-3}), q_{max} is the monolayer capacity of the adsorbent (mg g^{-1}), and b is the Langmuir adsorption constant (dm^3 g^{-1}). The Langmuir equation is based on the assumption of a structurally homogeneous adsorbent where all sorption sites are identical and energetically equivalent. The linearized form of this equation is the following:

$$c_e/q_e = 1/(q_{max}b) + c_e/q_{max} \quad (5)$$

Fig. 8 shows the straight-line plots of c_e/q_e vs. c_e for the adsorption of cyanocobalamine. The correlation coefficients are relatively high ranging from 0.947 to 0.984. The Langmuir constants calculated from the linear plot are given in Table 3. As can be seen the monolayer capacities of KJA/S/CaFe and KJA/Ti are comparable, around 50 mg g^{-1}. Over two-fold higher adsorption capacity (119 mg g^{-1}) is obtained for the KJA/N/CaFe carbon. A comparison of carbon's pore volume distribution (Fig. 3) indicates that the extent of adsorption is strongly related to the mesopore development. An increase in the adsorption capacity q_{max} with both the mesopore volume and the contribution of mesopore to the porous texture can be observed. Moreover, this is followed by an increase in the mean pore width that is a consequence of an increase in the volume of mesopores with a size of 10–50 nm.

The Freundlich model is applied to describe heterogeneous system characterized by a heterogeneity factor 1/n. This model describes reversible adsorption and is not restricted to the

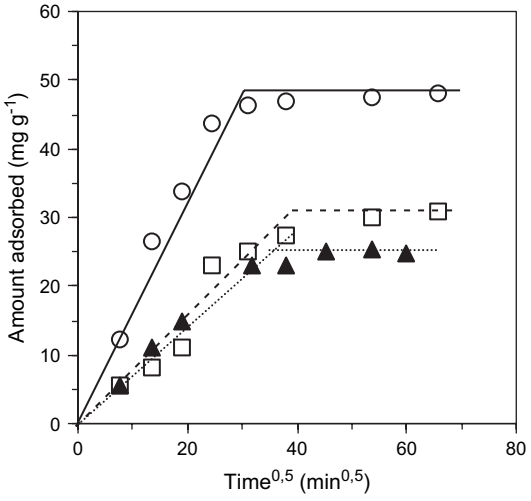

Fig. 6. Intraparticle diffusion plot for the adsorption of cyanocobalamine. ○, KJA/N/CaFe; □, KJA/S/CaFe; ▲, KJA/Ti.

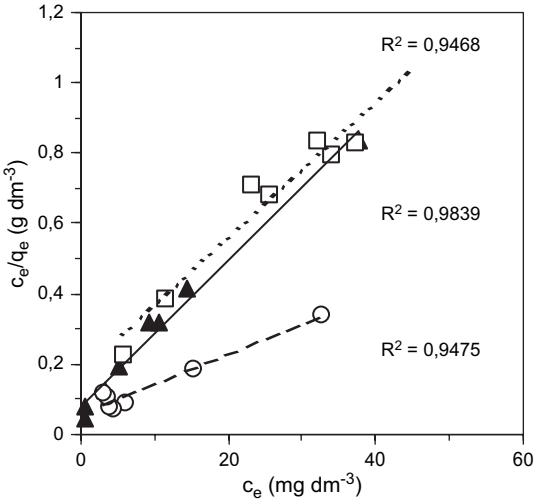

Fig. 8. Langmuir plots for adsorption of cyanocobalamine. ○, KJA/N/CaFe; □, KJA/S/CaFe; ▲, KJA/Ti.

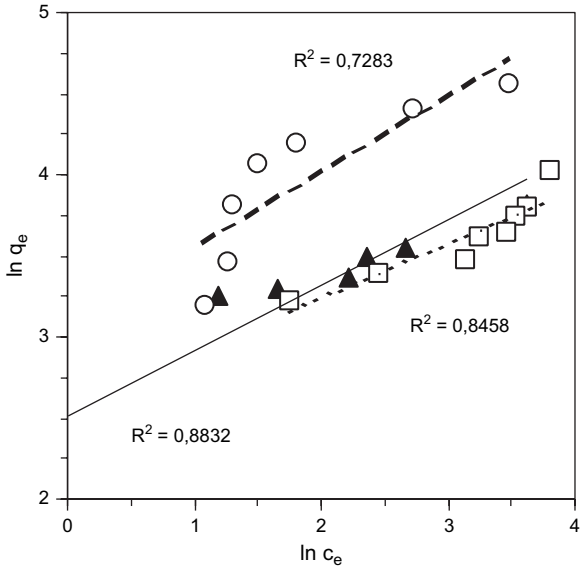

Fig. 9. Freundlich plots for adsorption of cyanocobalamine. ○, KJA/N/CaFe; □, KJA/S/CaFe; ▲, KJA/Ti.

formation of the monolayer. The Freundlich model is expressed by Eq. (6):

$$q_e = K_f c_e^{1/n} \quad (6)$$

where q_e and c_e are, respectively, the adsorbate equilibrium concentration on adsorbent (mg g^{-1}) and in solution (mg dm^{-3}) and K_f is the Freundlich constant (mg^{1-n} dm^{3n} g^{-1}). The Freundlich parameters K_f and $1/n$ were determined from the linear plots of $\log q_e$ vs. $\log c_e$ shown in Fig. 9. Their values are given in Table 3. A comparison of correlation coefficients R^2 indicates that the Langmuir model yields a better fit than the Freundlich model. Similarly to q_{max}, K_f that is related to the adsorption capacity increases with both the mesopore volume and the mesopore contribution. Considering three mesoporous carbons studied in this work the KJA/Ti carbon with the highest contribution of micropores shows the lowest ability to remove cyanocobalamine from aqueous solution.

4. Conclusions

A series of subbituminous coal-based mesoporous activated carbons with nearly the same total pore volume but different pore volume distribution was tested for the removal of cyanocobalamine from aqueous solution. The time required to attain the equilibrium is related to the degree of mesopore development. It can be observed that the equilibrium time decreases with increasing both the mesopore volume and the contribution of mesopores into the porous texture of carbon. The adsorption kinetics of cyanocobalamine on mesoporous carbons follows the pseudo-second-order model. It was found that the transport of the solute molecules from the aqueous phase to the external surface of carbon does not affect the rate of adsorption. The intraparticle diffusion is the only rate-controlling step.

The Langmuir isotherm model was found to provide a better prediction for the adsorption of cyanocobalamine than the Freundlich model. The Langmuir adsorption capacity of the carbon increases with the mesopore volume that is followed by increase in the volume of mesopores in size of 10–50 nm. The greatest efficiency in the removal of cyanocobalamine was obtained for the KJA/N/CaFe carbon which is characterized by the highest both the mesopore volume and the mean pore width. The obtained results prove that the mesopores play a crucial role in the removal of cyanocobalamine by adsorption.

Table 3
Langmuir and Freundlich parameters for cyanocobalamine adsorption on mesoporous activated carbons

Carbons	Langmuir		Freundlich	
	q_{max} (mg g^{-1})	b (dm^3 g^{-1})	K_f (mg^{1-n} dm^{3n} g^{-1})	$1/n$
KJA/N/CaFe	119	3.83	36	0.286
KJA/S/CaFe	51	7.30	15	0.419
KJA/Ti	48	8.31	16	0.299

References

[1] Forgacs E, Cserhati T, Oros G. Removal of synthetic dyes from wastewaters: a review. Environ Inter 2004;30:953–71.
[2] Robinson T, McMullan G, Marchant R, Nigam P. Remediation of dyes in textile effluent: a critical review on current treatment technologies with a proposed alternative. Bioresour Technol 2001;77:247–55.
[3] Lachheb H, Puzenat E, Houas A, Ksibi M, Elaloui E, Guillard C, et al. Photocatalytic degradation of various types of dyes (Alizarin S, Crocein Orange G, Methyl Red, Congo Red, Methylene Blue) in water by UV-irradiated titania. Appl Catal B Environ 2002;39:75–90.
[4] Wu CH. Comparison of azo dye degradation efficiency using UV/single semiconductor and UV/coupled semiconductor systems. Chemosphere 2004;57:601–8.

[5] Al-Degs Y, Khraisheh MAM, Allen SJ, Ahmad MN. Effect of carbon surface chemistry on the removal of reactive dyes from textile effluent. Water Res 2000;34:927–35.
[6] Chern JM, Wu CY. Desorption of dye from activated carbon beds: effects of temperature, pH, and alcohol. Water Res 2001;35:4159–65.
[7] Kannan N, Meenakshisundaram M. Kinetics and mechanism of removal of methylene blue by adsorption on various carbons – a comparative study. Dyes Pigments 2001;51:25–40.
[8] Faria PCC, Orfao JJM, Pereira MFR. Adsorption of anionic and cationic dyes on activated carbons with different surface chemistries. Water Res 2004;38:2043–52.
[9] Attia AA, Rashwan WE, Khedr SA. Capacity of activated carbon in the removal of acid dyes subsequent to its thermal treatment. Dyes Pigments 2006;69:128–36.
[10] Radovic LR, Moreno-Castilla C, Rivera-Utrilla J. Carbon materials as adsorbents in aqueous solution. In: Radovic LR, editor. Chemistry and physics of carbon, vol. 27. New York: Marcel Decker; 2001. p. 228–405.
[11] Moreno-Castilla C. Adsorption of organic molecules from aqueous solution on carbon materials. Carbon 2004;42:83–94.
[12] Radovic LR, Silva IF, Ume JI, Menendez JA, Leon Y Leon CA, Scaroni AW. An experimental and theoretical study of the adsorption of aromatics possessing electron-withdrawing and electron-donating functional groups by chemically modified activated carbons. Carbon 1997;35:1339–48.
[13] Nevskaia DM, Santianes A, Munoz V, Guerrero-Ruiz A. Interaction of aqueous solutions of phenol with commercial activated carbons: an adsorption and kinetic study. Carbon 1999;37:1065–74.
[14] Tamai H, Kakii T, Hirota Y, Kumamoto T, Yasuda H. Synthesis of extremely large mesoporous activated carbon and its unique adsorption for giant molecules. Chem Mater 1996;8:454–62.
[15] Tamai H, Yoshida T, Sasaki M, Yasuda H. Dye adsorption on mesoporous activated carbon fiber obtained from pitch containing yttrium complex. Carbon 1999;37:983–9.
[16] Lorenc-Grabowska E, Gryglewicz G. Adsorption of lignite-derived humic acids on coal-based mesoporous activated carbons. J Colloid Interface Sci 2005;284:416–23.
[17] Kannan N, Meenakshisundaram M. Adsorption of Congo Red on various activated carbons. Water Air Soil Pollut 2002;138:289–305.
[18] Namasivayam C, Kavitha D. Removal of Congo Red from water by adsorption onto activated carbon prepared from coir pith, an agricultural solid waste. Dyes Pigments 2002;54:47–58.
[19] Namasivayam C, Muniasamy N, Gayatri K, Rani M, Ranganathan K. Removal of dyes from aqueous solutions by cellulosic waste orange peel. Bioresour Technol 1996;57:37–43.
[20] Ho YS, McKay G. Pseudo-second order model for sorption processes. Process Biochem 1999;34:451–65.
[21] Bhattacharyya KG, Sarma A. Adsorption characteristics of the dye, Brilliant Green, on Neem leaf powder. Dyes Pigments 2003;57:211–22.
[22] Malik PK. Dye removal from wastewater using activated carbon developed from sawdust: adsorption equilibrium and kinetics. J Hazard Mater 2004;B113:81–8.
[23] Ho YS. Comment on ''Sorption of basic dyes from aqueous solution by activated sludge''. J Hazard Mater 2005;B114:241–5.
[24] Lorenc-Grabowska E, Gryglewicz G. Adsorption characteristics of Congo Red on coal-based mesoporous activated carbons. Dyes Pigments, in press.
[25] Lorenc-Grabowska E, Gryglewicz G, Gryglewicz S. Development of mesoporosity in activated carbons via coal modification using Ca- and Fe-exchange. Microporous Mesoporous Mater 2004;76:193–201.
[26] Yoshizawa N, Yamada Y, Furuta T, Shiraishi M, Kojima S, Tamai H, et al. Coal-based activated carbons prepared with organometallics and their mesoporous structure. Energy Fuels 1997;11:327–30.
[27] Gregg SJ, Sing KSW. Adsorption, surface area and porosity. London: Academic Press; 1997.
[28] Moreno-Castilla C, Rivera-Utrilla J, Lopez-Ramon MV, Carrasco-Marin F. Adsorption of some substituted phenols on activated carbons from a bituminous coal. Carbon 1995;33:845–51.
[29] Newcombe G, Drikas M. Adsorption of NOM onto activated carbon: electrostatic and non-electrostatic effects. Carbon 1997;35:1239–50.
[30] Hsieh C, Teng H. Influence of mesopore volume and adsorbate size on adsorption capacities of activated carbons in aqueous solutions. Carbon 2000;38:863–9.
[31] Ho YS, McKay G. Sorption of dye from aqueous solution by peat. Chem Eng J 1998;70:115–24.
[32] Kumar A, Kumar S, Kumar S. Adsorption of resorcinol and catechol on granular activated carbon: equilibrium and kinetics. Carbon 2003;41:3015–25.
[33] Ozcan AS, Ozcan A. Adsorption of acid dyes from aqueous solutions onto acid-activated bentonite. J Colloid Interface Sci 2004;276:39–46.